Computers & Structures Vol. 43, No. 2, pp. 373–384, 1992
Printed in Great Britain.

0045-7949/92 $5.00 + 0.00

SEISMIC BEHAVIOR OF BRIDGE PIERS INCLUDING SOIL–STRUCTURE INTERACTION

C. C. SPYRAKOS
Civil Engineering Department, West Virginia University, Morgantown, WV 26506-6101, U.S.A.

(*Received* 29 *January* 1991)

Abstract—As a rule, widely used practices do not consider soil–structure interaction (SSI) in the seismic design of bridges. This study attempts to assess the significance of SSI for the design of bridge piers placed on either a homogeneous deep soil stratum or a shallow soil stratum overlying a rigid bedrock. The objective is pursued through a simple, yet capable to capture the effects of the most crucial physical parameters, representation of a bridge pier–soil system. Cases in which SSI needs to be considered in the design are identified, and recommendations that can lead to more economical and safer bridge designs are provided.

NOTATION

a	radius of circular foundation
C_h	horizontal viscous damping coefficient for radiation soil damping
C_r	rocking viscous damping coefficient for radiation soil damping
C_s	shear wave velocity for the soil
E	Young's modulus for the pier
G	soil shear modulus
h	height of the pier
H	depth of soil stratum
I	moment of inertia about the weak axis of the pier
ζ	damping ratio of hysteretic structural damping
$\tilde{\zeta}$	damping ratio of equivalent system
ζ_h	damping ratio of viscous soil damping for lateral displacement
ζ_s	damping ratio of hysteretic soil damping
ζ_r	damping ratio of viscous soil damping for rocking motion
k	flexural stiffness of pier
k_h	horizontal stiffness of soil medium
k_r	rocking stiffness of soil medium
m	mass of bridge deck corresponding to one pier
M_r	moment at base of pier
p_h	horizontal force at the base of a pier
t	time variable
T	fundamental period of fixed base pier
$\tilde{T}$	fundamental period of equivalent system
u	relative lateral displacement of bridge deck
u_g	lateral ground displacement
$\ddot{u}_g$	lateral ground displacement of equivalent system
u_0	relative lateral displacement of pier base
u_t	total lateral displacement
V	base shear of fixed base pier
$\tilde{V}$	base shear of equivalent system
γ	Poisson's ratio for the soil
θ	rotation angle
ρ	soil mass density
ω	circular frequency of horizontal ground motion
$\omega_s, \omega_h, \omega_r$	circular frequencies pertaining to a fixed base pier

INTRODUCTION

Seismic design of bridges has been under continuous improvements since the 1971 San Fernando earthquake. Many research programs that have focused on studying the deficiencies of bridge designs during seismic excitations have lead to the development of both simple guidelines and elaborate design procedures [1–3]. Representative analysis and design approaches can be found in many comprehensive FHWA final reports [4–5].

Current practice usually follows the design procedures suggested by the AASHTO guide specifications [4]. According to well-defined bridge classifications, the AASHTO specifications recommend to use one of the following three methods of analysis; namely, the elastic seismic response coefficient, the single mode spectral analysis, and the multi-mode spectral analysis. Provisions are made to account for local soil–site effects, since they greatly affect the bridge behavior during strong ground motions. All three approaches are based on the postulation that the scattered field in the vicinity of the foundation and abutments plays a secondary role in influencing the bridge response. This inability of most current design procedures to account for soil–structure interaction can be attributed to numerous difficulties including the complexity of the problem, scarce pertinent experimental information and lack of a simple procedure that accounts for soil–structure interaction (SSI) in bridge design.

The objective of this study is to investigate the seismic performance of bridges including SSI. The emphasis is placed on studying the pier behavior, since piers together with the abutments are the most critical structural components in securing the integrity of bridges during earthquakes. The study also provides an assessment of the relative significance that bridge–soil system parameters play in designs that account for SSI. Based on this assessment, recommendations that can lead to more economical and safer bridge–pier designs are presented.

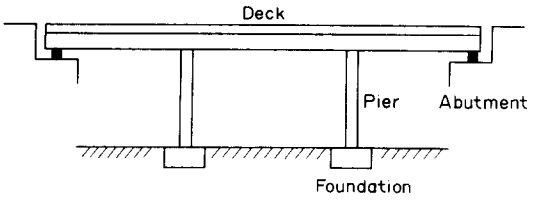

Fig. 1. Typical elevation of highway bridge.

BRIDGE–SOIL SYSTEM

The system considered is the idealized representation of a bridge excited along the longitudinal direction as shown in Fig. 1. In order to simplify the analysis, all piers are assumed to be massless, have equal lateral stiffness, and each one of them carries a portion of the deck mass denoted as m. The bridge deck is assumed to be substantially stiffer than the piers which may be either hinged or built-in to the girders. The assumption of a rigid deck greatly simplifies the dynamic analysis of the system by restricting the rotational degrees-of-freedom at the top of the piers with very little sacrifice in computational accuracy [2].

The soil supporting each pier through a massless circular foundation is modeled as spring–damper elements acting in the horizontal and rotational directions. The material damping in the soil is hysteretic with damping ratios ζ_g and ζ, respectively. The radiation damping representing loss of energy due to the infinite extent of the soil media is viscous with damping ratios ζ_h and ζ_r for the horizontal and rocking motions, respectively. Under these assumptions, the dynamic response of a pier with the corresponding part of the bridge deck can be simulated with the aid of the three-degrees-of-freedom model shown in Fig. 2(a). The three-degrees-of-freedom include the total lateral displacement of the bridge deck, u_t, the horizontal displacement of the foundation relative to the free-field motion, u_0, and the rotation of the system at the foundation level, θ.

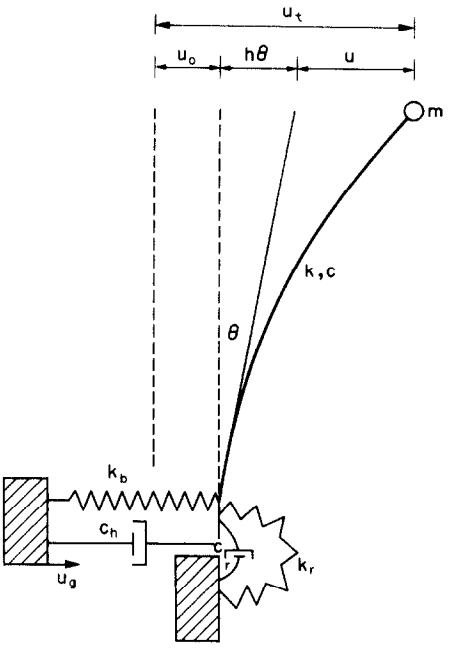

Fig. 2. Model of hinged-pier–soil system to horizontal excitation.

For a harmonic ground excitation, $u_g e^{i\omega t}$, the amplitudes of the horizontal force, P_h, and moment, M_r, that develop at the pier base can be written in the following form

$$P_h = k_h(1 + 2\zeta_h + {}^2\zeta_g^i)u_0$$

and

$$M_r = k_r(1 + 2\zeta_r + {}^2\zeta_g^i)\theta. \tag{1}$$

Equilibrium of the horizontal forces acting on m, as well as equilibrium of the horizontal forces and moments at the base of the pier lead to the equations of motion of the pier–soil system

$$\begin{bmatrix} \frac{\omega_s^2}{\omega^2}(1+2\zeta i)-1 & -1 & -\frac{1}{\alpha} \\ -1 & \frac{\omega_h^2}{\omega^2}(1+2\zeta_h i+2\zeta_g i)-1 & -\frac{1}{\alpha} \\ -1 & -1 & \begin{matrix}\frac{\alpha\omega_r^2}{\omega^2}(1+2\zeta_r i+2\zeta_g i)+ \\ \frac{(\alpha-1)}{3\alpha}\frac{\omega_s^2}{\omega^2}(1+2\zeta i)-\frac{1}{\alpha}\end{matrix} \end{bmatrix} \begin{Bmatrix} u \\ u_0 \\ h\theta \end{Bmatrix} = \begin{Bmatrix} u_g \\ u_g \\ u_g \end{Bmatrix}, \tag{2}$$

where

$$\omega_s^2 = \frac{3EI}{h^3}\alpha^2, \quad \omega_h^2 = \frac{k_h}{m}, \quad \omega_r = \frac{k_r}{mh^2} \tag{3}$$

and the parameter, α, is assigned the value of 1 for a hinged to the deck pier, and 2 for a built-in pier [1]. In eqn (2) and the ensuing formulation, the harmonic term, $e^{i\omega t}$ has been omitted for reasons of simplicity.

Only one of the three degrees of freedom in eqn (2) is dynamic, since all inertia effects except the horizontal lumped mass along the longitudinal direction of the bridge are neglected. Consequently,

the pier–soil response can be evaluated with the aid of an equivalent single degree-of-freedom system. The equation of motion of the equivalent single degree-of-freedom system is given by

$$\left(1+2\bar{\zeta}i-\frac{\omega^2}{\bar{\omega}^2}\right)u=\frac{\omega^2}{\bar{\omega}^2}\ddot{u}_g, \tag{4}$$

where

$$\bar{\omega}^2=\frac{1}{\dfrac{1}{\omega_s^2}+\dfrac{1}{\omega_h^2}+\dfrac{1}{\alpha^2\omega_r^2+[(a-1)/3]\,\omega_s^2}} \tag{5a}$$

$$\bar{\zeta}=\left(\frac{\bar{\omega}^2}{\omega_s^2}+\frac{(\alpha-1/3)\,\omega_s^2\bar{\omega}^2}{(\alpha^2\omega_r^2+[(\alpha-1)/3]\,\omega_2^2)^2}\right)$$

$$\times\zeta+\left(1-\frac{\bar{\omega}^2}{\omega_s^2}+\frac{(\alpha-1/3)\omega_s^2\bar{\omega}^2}{(\alpha^2\omega_r^2+[(\alpha-1)/3]\omega_s^2)^2}\right)\zeta_g$$

$$+\frac{\bar{\omega}^2}{\omega_s^2}\zeta_h+\frac{\alpha^2\bar{\omega}^2\omega_r^2}{(\alpha^2\omega_r^2+[(\alpha-1)/3]\,\omega_s^2)^2}\zeta_r, \tag{5b}$$

and

$$\ddot{u}_g=\frac{\bar{\omega}^2}{\omega_s^2}\ddot{u}_g. \tag{5c}$$

The equivalent single degree-of-freedom has been derived under the assumptions of maintaining the same mass, m, with the three-degrees-of-freedom system governed by eqn (3), and by enforcing equal relative displacement amplitudes, u, at resonance in both the single-degree and the three-degrees-of-freedom systems. The equivalent damping ratio, $\bar{\zeta}$, has been evaluated a resonance, i.e., $\bar{\omega}=\omega$, and then used for the whole frequency range [1]. The concise expressions of the equivalent single degree-of-freedom system facilitate the understanding of the influence that SSI has on the seismic behavior of bridge structures, and allow to easily identify the relative significance that the various parameters play in affecting the system response.

PIER–SOIL SYSTEM AND METHOD OF ANALYSIS

Contrary to stiffness and damping in bridge super- and sub-structures, soil stiffness and damping depend on the frequency content of seismic excitations. For design purposes, however, a sufficiently accurate consideration of soil behavior can be obtained if the soil stiffness and damping coefficients of a circular massless foundation on soil strata are evaluated by the following frequency independent expressions [6]:

$$k_h=\frac{8Ga}{2-\gamma}\left(1+\frac{1}{2\bar{H}}\right)\quad\text{for}\quad\bar{H}>1,$$

$$k_h=\frac{8Ga^3}{3(1-\gamma)}\left(1+\frac{1}{6\bar{H}}\right)\quad\text{for}\quad 1<\bar{H}\leqslant 4,$$

$$c_h=\frac{4.6Ga^2}{(2-\gamma)c_s},$$

and

$$c=\frac{0.4Ga^4}{(1-\gamma)c_s}, \tag{6}$$

where, a, is the radius of the circular foundation, H is the depth of the soil stratum overlying a rigid bedrock and $\bar{H}=H/a$. The above expressions are also valid for the limiting case of a very deep soil stratum, in which case the terms involving $\bar{H}$ diminish. The effects of SSI on the bridge–pier–soil system subjected to a harmonic seismic excitation can be better understood by expressing the system dynamic properties in terms of the dimensionless parameters

$$\bar{p}=\frac{3EI}{Gh^3a}\alpha^2,\quad\bar{h}=\frac{h}{a},\quad\text{and}\quad\bar{m}=\frac{m}{\rho a^3}. \tag{7}$$

The salient parameters that characterize the effects of SSI are the ratio of period of the equivalent system, $\bar{T}$, to the period of the fixed base pier–bridge deck structure, T, and the shear reduction factor $\bar{V}/V$. The ratio $\bar{T}/T$, can be deduced from eqn (5a) to obtain

$$\frac{\bar{T}}{T}=\left[1+\frac{\omega_s^2}{\omega^2}+\frac{1}{\alpha^2\omega_r^2+(\alpha-1/3)\,\omega_s^2}\right]^{1/2}. \tag{8}$$

The shear reduction factor is discussed in a separate section of this work. In view of eqns (6), eqns (8) and (5b) can be expressed as

$$\frac{\bar{T}}{T}=\left[1+\frac{\bar{p}}{8}\left(\frac{2-\gamma}{\left(1+\dfrac{1}{2\bar{H}}\right)}\right.\right.$$

$$\left.\left.+\frac{24(1-\gamma)\bar{h}^2}{8\alpha^2\left(1+\dfrac{1}{6\bar{H}}\right)+(\alpha-1)(1-\gamma)\bar{p}\bar{H}^2}\right)\right]^{1/2} \tag{9}$$

and

$$\bar{\zeta}=D_s+D_m+D_r, \tag{10}$$

where

$$D_s = \left(\frac{T}{\bar{T}}\right)^2 \left[1 + \frac{3(\alpha-1)(1-\gamma)^2\bar{p}^2\bar{h}^4}{64\alpha^4\left(1+\frac{1}{6\bar{H}}\right)^2 + 16\alpha^2(\alpha-1)(1-\gamma)\left(1+\frac{1}{6\bar{H}}\right)\bar{p}\bar{h}^2(\alpha-1)^2(1-\gamma)^2\bar{p}^2\bar{h}^4}\right]\zeta$$

$$D_m = \left[1 - \left(\frac{T}{\bar{T}}\right)^2 \left[1 + \frac{3(\alpha-1)(1-\gamma)^2\bar{p}^2\bar{h}^4}{64\alpha^4\left(1+\frac{1}{6\bar{H}}\right)^2 + 16\alpha^2(\alpha-1)(1-\gamma)\left(1+\frac{1}{6\bar{H}}\right)\bar{p}\bar{h}^2(\alpha-1)^2(1-\gamma)^2\bar{p}^2\bar{h}^4}\right]\right]\zeta_g. \quad (11)$$

and

$$D_r = \left(\frac{T}{\bar{T}}\right)^3 \sqrt{\left(\frac{\bar{p}^3}{m}\right)}\left[\frac{4.6}{12\zeta}(2-\gamma)\frac{1.8\alpha^2(1-\gamma)\bar{h}^2}{64\alpha^4 + 16\alpha^2(\alpha-1)(1-\gamma)p\bar{h}^2 + (\alpha-1)^2(1-\gamma)^2p^2\bar{h}^4}\right]. \quad (12)$$

In eqn (9), the first two terms pertain to material damping in the structure and the soil, respectively, while the third term is associated with radiation damping in the soil. It should be noted that if $H < 5a$ and $T > 4H/c_s$, the contribution of radiation damping in the soil is insignificant and the term D_r can be ignored in the analysis [6].

ASSESSMENT OF SSI EFFECTS

Equivalent period and damping ratio

In order to assess the effects of SSI on bridge–soil systems a series of parametric studies have been performed. They all refer to a girder hinged to the bridge deck and supported by either a homogeneous semi-infinite soil medium or a shallow soil stratum overlying a rigid bedrock. Figure 3 depicts the variation of $\bar{T}/T$ as a function of $\bar{p}$ for representative values of $\bar{h}$. For the evaluations shown in Fig. 3 and all the subsequent figures, a Poisson's ratio $\gamma = 0.4$ has been selected for the soil. As expected, by either decreasing the soil stiffness or increasing the slenderness of the structure results in increasing $\bar{T}/T$. Since variations of the ratio $\bar{T}/T$ in terms of the soil–pier physical parameters can be regarded as characterizing the effect of soil–structure interaction, it can be deduced that for stiff bridge piers placed on flexible soil, SSI causes substantial changes in the fundamental period of the system and should be considered in design. Further, an increase of the pier height not followed by an appropriate increase of the foundation dimensions leads to augmentation of the SSI effects.

In Figs 4(a–c) the variation of the three components of equivalent damping corresponding to structural material damping, D_{sh}, soil material damping, D_{mh}, and soil radiation damping, D_{rh}, are plotted versus $\bar{p}$ for representative values of $\bar{h}$, and $\bar{m}$. The subscript, h, denotes the damping parameters that refer to a pier hinged to the deck, and have been evaluated from eqns (11) and (12) for $\alpha = 1$. The structural material damping ratio ζ and the soil material damping ratio ζ_g are selected to be 0.05 and 0.08, respectively. The selected value of ζ characterizes reinforced concrete piers, while the value of ζ_g represents a realistic value of hysteretic soil damping during strong ground motions. Decreasing

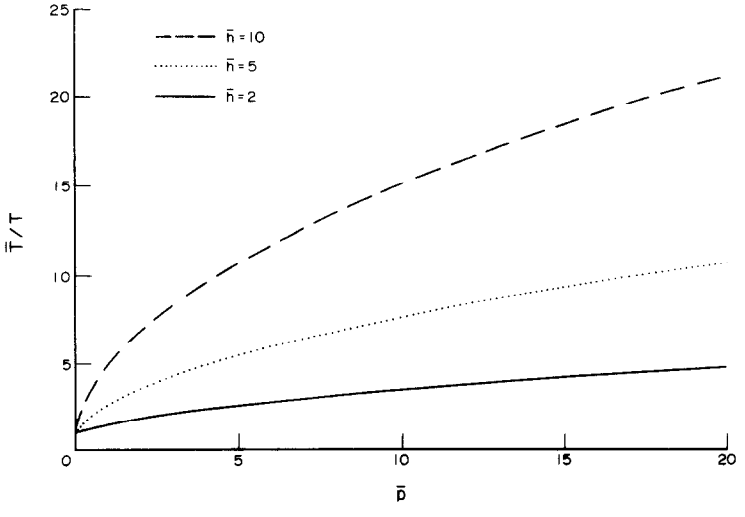

Fig. 3. Fundamental period ratio of pier on deep soil medium.

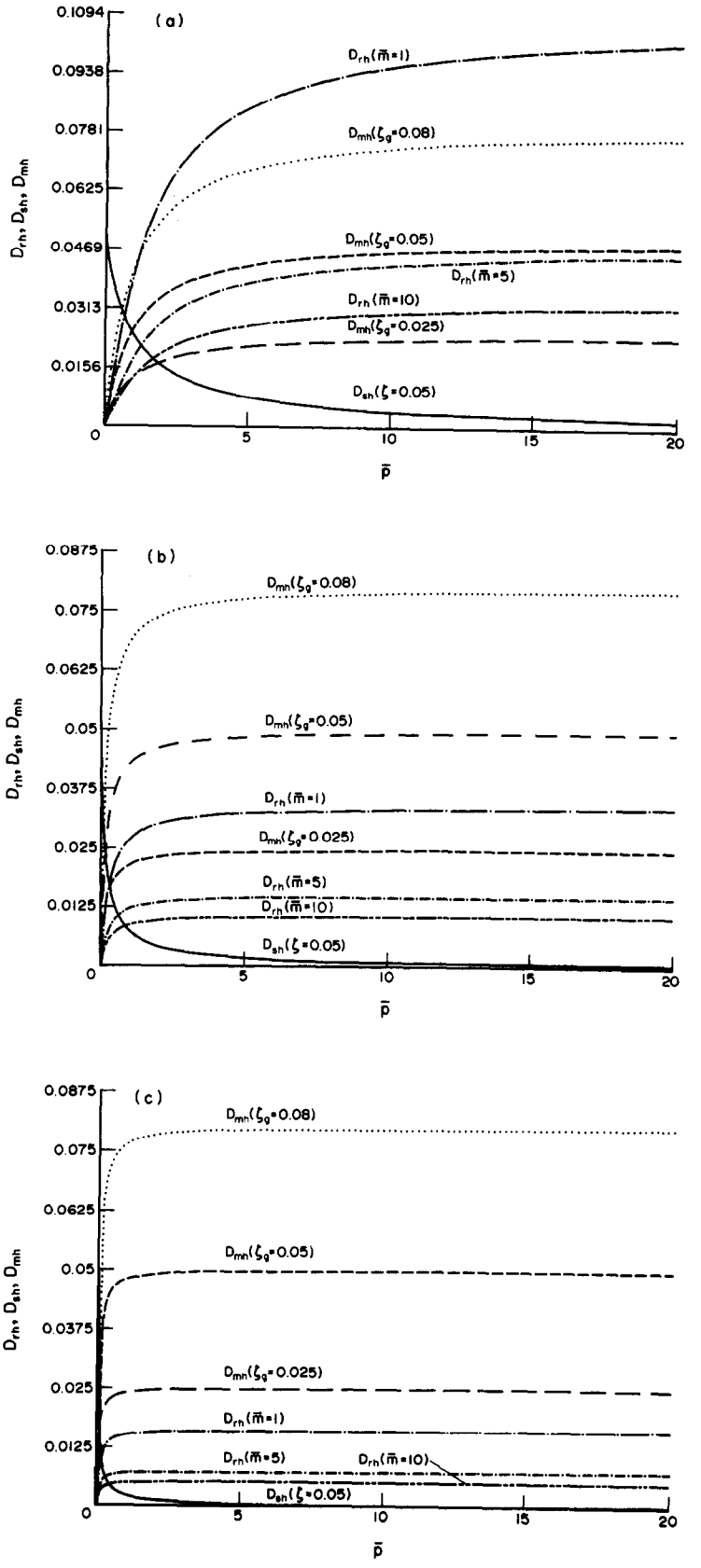

Fig. 4. (a) Variation of damping components for $\bar{h} = 2$. (b) Variation of damping components for $\bar{h} = 5$. (c) Variation of damping components for $\bar{h} = 10$.

the soil stiffness results in a decrease of the structural material damping contribution D_{sh} and an increase of the soil material damping D_{mh}. If the structural material damping ratio ζ is equal to the soil material damping ratio ζ_g, the combination of D_{sh} and D_{mh} becomes constant and equal to ζ. The contribution of both D_{sh} and D_{mh} will lead to an increase of $\bar{\zeta}$ as the soil becomes more flexible for ζ_g being greater than ζ, and will lead to a decrease of $\bar{\zeta}$ for ζ_g smaller than ζ. Also, referring to the curves $D_{sh}(\zeta = 0.05)$, $D_{mh}(\zeta_g = 0.025)$, $D_{mh}(\zeta_g = 0.05)$ and $D_{mh}(\zeta_g = 0.08)$ of Figs. 4, it is observed that the rates at which the soil material damping contribution decreases are moderately influenced by the slenderness ratio $\bar{h}$. For slender piers in which the rocking motion is predominant, soil material damping increases sharply and approaches its maximum value of ζ_g for low values of $\bar{p}$; such a behavior clearly indicates the significance that soil material damping can play on slender structures. However, structural material damping decreases and approaches zero at low values of $\bar{p}$. Thus, in slender piers on flexible soil the equivalent damping is mostly attributed to soil damping. For squat piers corresponding to large values of $\bar{p}$, the rate of change of both the D_{mh} and D_{sh} is smaller than that in slender piers. It should be noted that, for both squat and slender piers, soil material damping contribution approaches the total soil material damping ratio ζ_g and the structural material damping contribution becomes negligible as the soil stiffness decreases. This is anticipated since, when the soil stiffness is small compared to the pier stiffness, the deformation of the equivalent one-degree-of-freedom system becomes mostly soil deformation resulting in an increase of soil material damping. In that case the pier can be regarded as a rigid bar rocking about its base without any deformation and, hence, without any structural material damping.

From the curves pertaining to radiation damping and designated with D_{rh} in Fig. 4, it is observed that the radiation damping is higher for small values of the mass ratio $\bar{m}$. Since radiation damping is a function of the structural mass, soil density and footing dimensions, higher radiation damping can be obtained by increasing the soil density, by decreasing the structural weight or finally by increasing the foundation contact area with the soil, while maintaining the pier height unchanged. Also, any decrease in soil stiffness results in increasing the radiation damping. From all alternatives, an increase in the dimensions of the foundations plays the most significant role in enhancing radiation damping with regard to the effect of slenderness ratio. The curves D_{rh} ($\bar{m} = 1$), D_{rh} ($\bar{m} = 5$) and D_{rh} ($\bar{m} = 10$) in Fig. 4 depict that radiation damping effects are more significant for squat rather than slender piers. The three components of the equivalent damping, i.e., D_{sh}, D_{mh}, D_{rh} are added, and plotted as a function of $\bar{p}$, with $\zeta_g = 0.08$ and $\bar{m} = 1$, 5, 10, for $\bar{h} = 2,5$, and 10 in Figs 5(a–c), respectively. The significance of the radiation damping contribution is clearly depicted in Fig. 5. In order to gauge this contribution, the variation of $\bar{\zeta}$ for zero radiation damping $D_r = 0$ has been plotted for each representative value of the slenderness ratio $\bar{h}$. If radiation damping is considered, the equivalent damping $\bar{\zeta}$ is larger to squat piers than in slender piers. This should be mostly attributed to the radiation damping which, as mentioned earlier, is more significant for squat piers. If radiation damping is not considered, as in curve $D_r = 0$, $\bar{\zeta}$ is slightly higher in slender piers than in squat piers. In Figs 5(a–c), the equivalent damping $\bar{\zeta}$ is always greater than the fixed base structural damping, ζ. It is worth noting, as indicated by eqn (10), that when there is no radiation damping and the soil material damping ratio ζ_g is smaller than the structural damping ratio ζ, the equivalent damping $\bar{\zeta}$ will be smaller than the fixed-base structural damping ζ.

When the bridge is founded on a shallow soil stratum overlying a rigid bedrock, several significant changes of the pier behavior are observed comparing to the case of a supporting semi-infinite soil. In Fig. 6, $\bar{T}/T$ is plotted as a function of $\bar{p}$ for $\bar{H} = 1$, 4 and several representative values of $\bar{h}$. Similarly to the semi-infinite soil case, decreasing the stiffness of the soil results in an increase of $\bar{T}/T$. It is also observed that the effect of $\bar{H}$ is very small compared to the effect of the slenderness ratio $\bar{h}$. The increase in slenderness ratio leads to larger values of $\bar{T}/T$ and therefore soil–structure interaction effects are more pronounced in slender piers. From eqn (9), it can be deducted that when the soil material damping ratio ζ_g is equal to the structural material damping ζ, a constant equivalent damping $\bar{\zeta}$ equal to ζ is obtained, and when ζ_g is less than ζ, the equivalent damping will decrease for increasing $\bar{p}$. In Fig. 7, the equivalent damping $\bar{\zeta}$ is plotted as a function of $\bar{p}$ for $\bar{H} = 1$, 4, and $\bar{h} = 2$, 5, and 10. It is observed that $\bar{H}$ has a negligible effect on the equivalent damping ratio. This is attributed to the substantial reduction of damping which in turn is imposed by the rigid bedrock that restricts the emanation of waves away from the shallow stratum. At low values of $\bar{p}$, the equivalent damping $\bar{\zeta}$ presents a sharper increase in slender piers than that in squat piers. Further, the slenderness ratio effects diminish as the soil stiffness decreases.

Seismic base shear

When the effects of soil–structure interaction are neglected, the shear at the base of the pier can be evaluated as recommended by the current Guide Specification of Seismic Design of Highway Bridges [4]

$$V = C_s W, \tag{13}$$

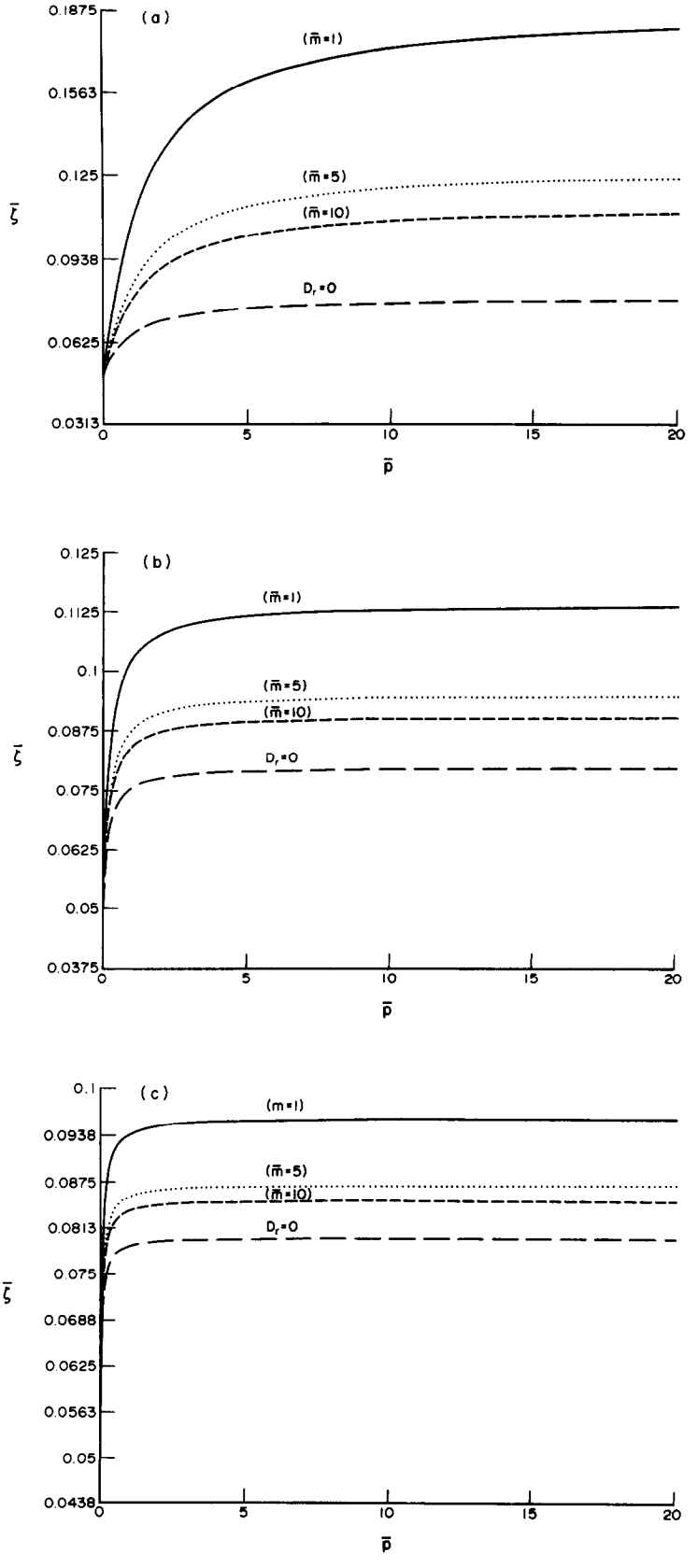

Fig. 5. (a) Equivalent damping ratio for deep soil medium and $\bar{h} = 2$. (b) Equivalent damping ratio for deep soil medium and $\bar{h} = 5$. (c) Equivalent damping ratio for deep soil medium and $\bar{h} = 10$.

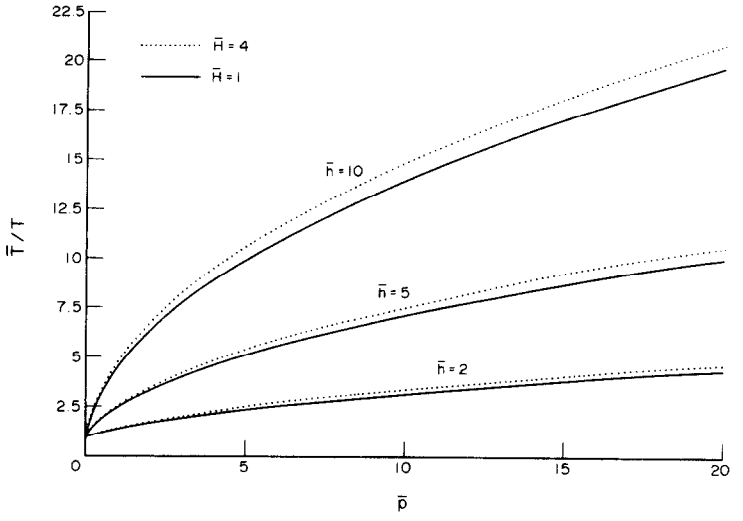

Fig. 6. Fundamental period ratio of pier on shallow soil stratum.

where W is the gravity weight associated with the pier and the seismic design coefficient, C_s, can be evaluated from

$$C_s(T,\zeta)=1.2\frac{AS}{T^{2/3}}. \tag{14}$$

As equation (14) indicates, $C_s(T,\zeta)$ depends on the fundamental period of the fixed base structure, T, the effective peak velocity-related acceleration coefficient A, and accounts for both structural damping and local soil conditions through the dimensionless site coefficient, S. It should be clarified though that S does not account for SSI effects. Introducing a $C_s(\bar{T},\bar{\zeta})$ that considers SSI, the shear at the base of the pier could be determined from

$$\bar{V}=C_s(\bar{T},\bar{\zeta})W. \tag{15}$$

In eqn (15), $C_s(\bar{T},\bar{\zeta})$ should be evaluated from the fundamental period and damping ratio of the equivalent one-degree-of-freedom system with natural period, $\bar{T}$, and damping ratio, $\bar{\zeta}$. Assuming initially that the damping of the system is ζ and the period is $\bar{T}$, eqn (14) renders the following expression for $C_s(\bar{T},\zeta)$

$$C_s(T,\zeta)=1.2\frac{AS}{\bar{T}^{2/3}}. \tag{16}$$

For the most commonly encountered soil conditions subjected to medium to strong intensities of seismic ground motions, $C_s(\bar{T},\bar{\zeta})$ can be related to $C_s(\bar{T},\zeta)$ through the relationship [7]

$$C_s(\bar{T},\bar{\zeta})=C_s(\bar{T},\zeta)\left(\frac{\zeta}{\bar{\zeta}}\right)^{0.4}. \tag{17}$$

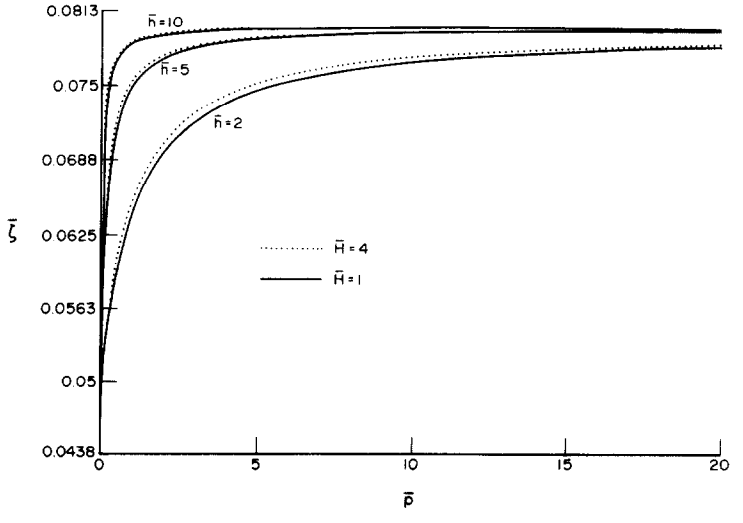

Fig. 7. Equivalent damping ratio of pier on shallow soil stratum.

In view of eqns (15)–(17), the ratio of the base shear accounting for SSI, $\bar{V}$, to the fixed base shear, V, as specified by the current AASHTO recommendations, can be determined from

$$\frac{\bar{V}}{V} = \left(\frac{T}{\bar{T}}\right)^{2/3} \left(\frac{\zeta}{\bar{\zeta}}\right)^{0.4}. \tag{18}$$

The shear reduction factor, $\bar{V}/V$, can be expressed in terms of the previously defined dimensionless parameters, $\bar{p}$, $\bar{h}$, $\bar{m}$, and $\bar{H}$, in order to assess the effect that accounting for SSI may have on the current AASHTO design procedures.

The case of a hinged pier supported by a circular foundation on a homogeneous semi-infinite soil is studied first. The shear reduction factor $\bar{V}/V$ in eqn (18) can be expressed as a function of the previously defined dimensionless parameters $\bar{p}$, $\bar{h}$, $\bar{m}$, and $\bar{H}$. Figures 8(a–c), depict the variation of $\bar{V}/V$ as a function of $\bar{p}$ for representative values of $\bar{m}$ and $\bar{h}$. The structural material damping ζ and the soil material damping ζ_s are assumed to be 0.05 and 0.08, respectively. As expected, Fig. 8 clearly indicates that the pier base shear decreases when the soil stiffness is decreasing. However, a decrease in soil stiffness usually leads to an increase of the total horizontal displacement at the top of the pier relative to the base, which in turn may increase the secondary shear associated with P–δ effects. Such an increase is generally small and is usually neglected in analysis [3]. Starting from small values of $\bar{p}$, the shear reduction factor presents a sharp decrease. Such a behavior clearly indicates that appropriate exploitation of SSI can lead to more economical and safer bridge designs. Figure 8 also indicates that the effect of the mass ratio $\bar{m}$ on $\bar{V}/V$ is more apparent in bridges supported by short stiff piers and can be primarily attributed to an associated increase of radiation damping. For small values of $\bar{m}$, which pertain to either a small bridge mass, firm soil conditions and/or large dimensions of the foundation, a greater reduction in shear is obtained. For slender piers, the effect of $\bar{m}$ on $\bar{V}/V$ is

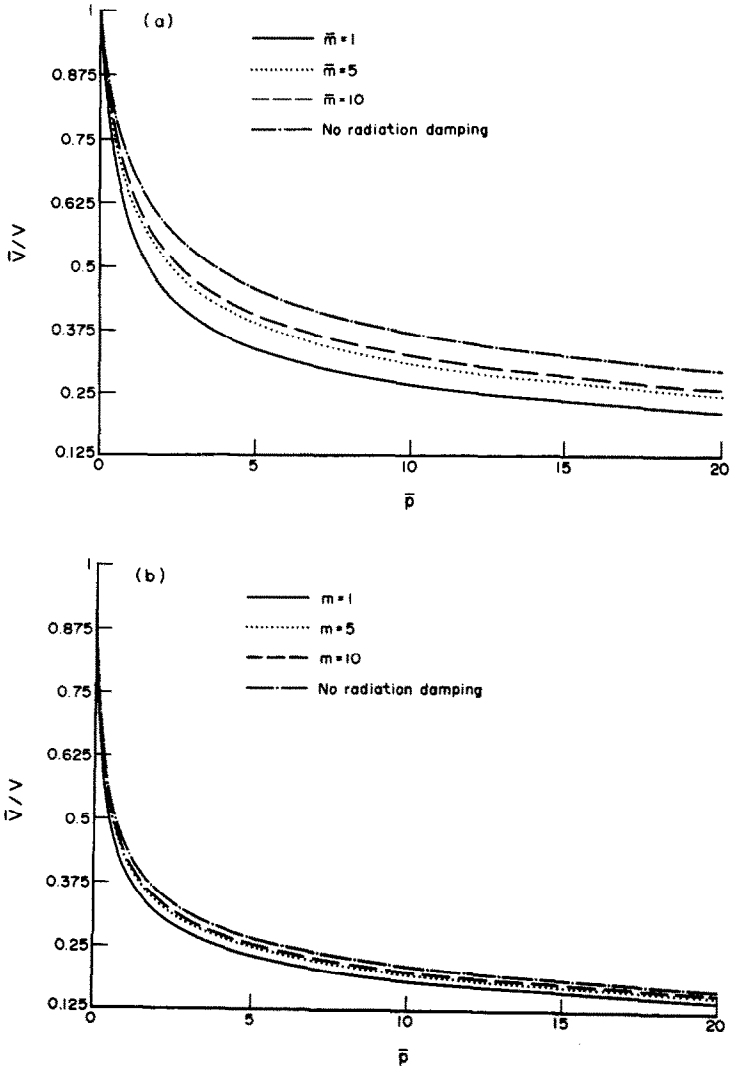

Fig. 8(a,b)—*Caption overleaf.*

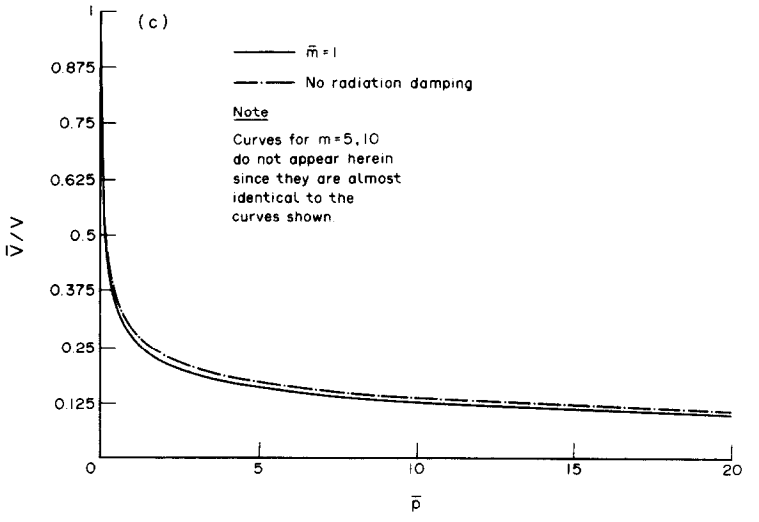

Fig. 8(c).

Fig. 8. (a) Shear force reduction factor for $\bar{h}=2$ and a deep soil stratum. (b) Shear force reduction factor for $\bar{h}=5$ and a deep soil stratum. (c) Shear force reduction factor for $\bar{h}=10$ and a deep soil stratum.

small and could be neglected in the design. Finally by comparing Figures 8(a–c), it can be inferred that the reduction in the base shear due to soil–structure interaction is more significant in tall piers.

Equation (18) is also valid for bridge piers with circular foundations placed on a shallow stratum overlying a rigid bedrock. Figure 9 depicts the variation of $\bar{V}/V$ as a function of $\bar{p}$ for several representative values of $\bar{H}$ and $\bar{h}$. As in the case of a hinged pier placed on a semi-infinite soil, decreasing the soil stiffness results in smaller values of $\bar{V}/V$. The decrease in $\bar{V}/V$ is characterized by the slenderness ratio $\bar{h}$. Namely, at low values of $\bar{p}$, the decrease of $\bar{V}/V$ in slender piers is sharper than that in short piers. By comparing the solid and dotted curves, it can be deduced that the variation of $\bar{H}$ has an insignificant effect on $\bar{V}/V$, and thus it can be neglected in the design of bridge piers.

NUMERICAL EXAMPLES

As a representative example, a three span continuous box-girder bridge with two seat-type abutments and two piers each of which is a three-column bent has been selected to demonstrate the effects of accounting for SSI in analysis. The box-girder is constructed monolithically with the bents. The configuration and member sizes of the bridge can be found in Appendix A of the AASHTO Guide Specifications [4]. Herein only the properties that are necessary to perform the analysis are presented; namely, the modulus of elasticity of a

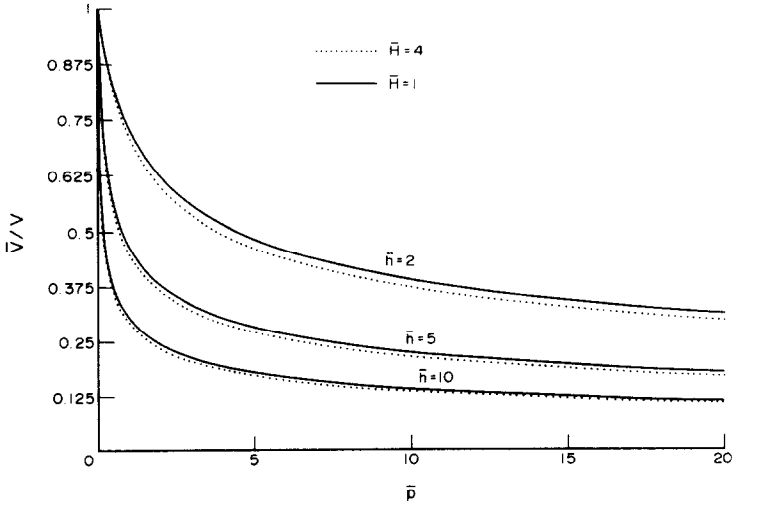

Fig. 9. Shear force reduction factor of pier on shallow soil stratum.

Table 1. Shear ratio $\bar{V}/V$

		Hinged pier			Built-in-pier		
		$a = 48$ in	$a = 96$ in	$a = 144$ in	$a = 48$ in	$a = 96$ in	$a = 144$ in
$G = 50{,}000$ psi	$Dr = 0$	0.858	0.975	0.992	0.856	0.970	0.988
	$Dr \neq 0$	0.856	0.975	0.991	0.862	0.967	0.985
$G = 20{,}000$ psi	$Dr = 0$	0.741	0.943	0.980	0.775	0.932	0.970
	$Dr \neq 0$	0.738	0.940	0.978	0.769	0.923	0.961
$G = 2000$ psi	$Dr = 0$	0.399	0.697	0.849	0.588	0.706	0.808
	$Dr \neq 0$	0.395	0.677	0.818	0.570	0.653	0.718

column $E = 30 \times 10^6$ psi, the column bent moment of inertia and height $I = 269{,}568$ (in^4) and $h = 300$ (in), respectively, and the bridge mass associated with one column bent $m = 3292.3$ (lb sec^2/in). The deck–pier–soil model is similar to the one shown in Fig. 2.

In order to enunciate the influence that SSI can have on the design of bridge piers, several parameters that affect the bridge response and are pertinent to SSI have been varied. The parameters varied include: the soil stiffness, the dimensions of the foundation and the rigidity of the bridge deck connection. The last parameter is studied for the two limiting cases of either a built-up or a hinged-deck–pier configuration. In order to assess the contribution of radiation damping, the evaluations have been performed for the cases of either including or excluding radiation damping. The results of the parametric studies are presented in Table 1.

The results reaffirm the remarks presented in the parametric studies, and clearly illustrate the significant contribution of SSI in reducing the base shear when the relative stiffness between the structure and the soil is decreased. They also depict the important role that radiation damping can play when the foundation size is increased and/or the soil stiffness is decreased. Observing the effect that the degree of fixidity between the deck and the pier plays on the bridge response, it can be asserted that an increase in the deck–pier fixidity lessens the effects of SSI on the seismic bridge response. Extensive parametric studies and additional representative examples can be found in the work of Al-Deghaither [1].

CONCLUSIONS

The effects of soil–structure interaction on the response of bridge piers placed either on a deep or shallow soil strata and subjected to horizontal seismic excitations have been studied.

The pier–soil system behavior is investigated through simple, yet capable to capture the salient features of soil structure interaction, structure–soil idealizations. The emphasis has been placed on gauging the relative significance that physical parameters play in affecting the system response, and on identifying when consideration of SSI leads to substantial differences from current design practices.

A thorough study of the system behavior with the aid of simple models has lead to: first, assess the effect of SSI on the seismic behavior of bridge piers; second, provide criteria that can be used in preliminary designs to decide whether SSI should be accounted for; and third, evaluate the shear in the piers including SSI with an-easy-to-use design procedure.

Extensive parametric studies have demonstrated that by considering SSI in bridge designs an enhancement of pier seismic behavior and the significant decrease of structural stresses leading to reduction in design costs could be duly accounted for.

Acknowledgements—The authors are thankful to the West Virginia Department of Highways and the U.S. Department Transportation for supporting this study under the Transportation Centers Program.

REFERENCES

1. S. Al-Deghaither, Seismic response of bridge piers including soil–structure interaction. MCSE Problem Report, Civil Engineering Department, West Virginia University, Morgantown, WV (1988).
2. C. B. Crouse, B. Hushmand and G. R. Martin, Dynamic soil–structure interaction of a single span bridge. *Earthquake Engng Struct. Dyn.* **15**, 711–729 (1987).
3. S. Okamoto, *Introduction to Earthquake Engineering*. University of Tokyo Press, Tokyo (1984).
4. American Association of State Highway and Transportation Officials, (AASHTO), Guide specification for seismic design of highway bridges (1983).
5. Federal Highway Administration, Seismic design and retrofit manual for highway bridges, Report No. FHWA-IP-87-6 (1987).
6. G. Gazetas, Analysis of machine foundations: state of the art. *Soil Dyn. Earthquake Engng* **2**, 1–42 (1983).
7. A. S. Veletsos and V. V. Nair, Seismic interaction of structures on hysteretic foundations. *J. Struct. Div., ASCE* **101**, 109–129 (1975).
8. H. V. S. GangaRao, Research in vibration analysis of highway bridges. *Shock Vibr. Digest* **6**, 17–22 (1984).
9. A. Ghobarah and H. M. Ali, Seismic performance of highway bridges. *Engng Struct.* **10**, 157–166 (1988).
10. D. Somaini, Seismic behavior of girder bridges for horizontally propagating waves. *Earthquake Engng Struct. Dyn.* **15**, 777–793 (1987).
11. C. C. Spyrakos and H. Antes, Time domain boundary element method approaches in elastodynamics: a comparative study. *Comput. Struct.* **24**, 529–535 (1986).

12. C. C. Spyrakos, Dynamic behavior of foundations in bilateral and unilateral contact. *Shock Vibr. Digest* **20,** 3–12 (1988).
13. L. C. Wilson, Analysis of the observed seismic response of a highway bridge. *Earthquake Engng Struct. Dyn.* **14,** 339–354 (1986).
14. J. P. Wolf, *Dynamic Soil–Structure Interaction.* Prentice-Hall, Englewood Cliffs, NJ (1985).